ADAPTIVE QUANTIZATION BY SOFT THRESHOLDING IN HEVC

Lee Prangnell [1], Victor Sanchez [1], and Rahul Vanam [2]
[1] Department of Computer Science, University of Warwick, Coventry, England, UK
[2] InterDigital Communications, Inc., San Diego, California, USA

Abstract—**The High Efficiency Video Coding (HEVC) reference encoder includes a Uniform Reconstruction Quantization (URQ) method. This block level quantization technique does not take into account the importance of transform coefficients in terms of signal reconstruction. In this paper, we present a transform coefficient level quantization technique based on a *soft thresholding* approach, in which the quantization parameter (QP) of a transform coefficient is altered according to its importance in the signal reconstruction process and according to the overall energy of the corresponding Transform Block (TB). The proposed method attains important coding efficiency performance gains as measured by the Bjøntegaard Delta Bitrate metric (BD-Rate). In comparison with reference encoder HM 16, our technique produces both luma and chroma BD-Rate improvements in all JCT-VC test sequences, particularly for sequences in Class E using the Low Delay B and Low Delay P configurations, with BD-Rate reductions of up to 5.5% (Y), 13.2% (Cb) and 11.7% (Cr).**

Keywords—HEVC; DCT; adaptive quantization; soft thresholding.

I. INTRODUCTION

The Joint Collaborative Team on Video Coding (JCT-VC) recently standardized HEVC. In comparison with the previous video coding standard developed by ITU-T/ISO/IEC, Advanced Video Coding (H.264/MPEG-4 AVC), HEVC has been shown to yield considerable bitrate savings, of approximately 50%, while preserving visual quality [1]. Similar to previous block-based hybrid video coding standards, the HEVC standard applies — after intra or inter prediction and linear transformation by the Discrete Cosine Transform (DCT) — quantization on transform coefficients to achieve lossy compression. The default quantization method in HEVC is URQ [1]. URQ, which is typically used in combination with Rate Distortion Optimized Quantization (RDOQ), is a block level quantization approach that equally quantizes all transform coefficients in a TB according to a QP value [2].

Transform coefficients within a TB are obtained after applying a finite precision approximation of the DCT on prediction residual values. These coefficients consist of low frequency, or high energy, transform coefficients and high frequency, or low energy, transform coefficients. Since most of the energy in a TB is concentrated in the low frequency components, the low frequency transform coefficients are more important than the high frequency components in terms of signal reconstruction and visual quality. URQ does not take into account the importance of transform coefficients, which constitutes an important shortcoming of this quantization method.

Alternative HEVC quantization methods have been previously proposed to improve upon URQ. In [3], a Structural Similarity Index Metric (SSIM) based adaptive quantization technique is proposed. The method selects specific QP values for blocks in the spatial domain based on optimizing the SSIM of an entire picture. The work in [4] proposes an Intensity Dependent Spatial Quantization (IDSQ) technique, which is designed to perceptually and adaptively adjust quantization by exploiting intensity masking of the human visual system. In [5], the authors propose Adaptive Quantization for Screen Content Videos (AQSCV), which is based on Rate Distortion Optimization (RDO). AQSCV functions with or without transform coefficients; it works in both the spatial domain — with bilateral filters from preventing artifacts across boundaries — and the frequency domain. An N-Level Quantizer is proposed in [6], which employs a coefficient level quantization method. This technique is based on hard thresholding quantization; it changes the QP value of transform coefficients according to their position in the TB scanning order used for entropy coding [6].

In this paper, we propose a novel quantization technique based on a coefficient level, smaller quantization step size scheme for low frequency components in a TB. More specifically, the proposed technique uses an adaptive, *soft thresholding* method to quantize coefficients according to their contribution to the reconstruction quality of the signal. In our technique, the QP of a transform coefficient is altered according to its position in relation to its Euclidean distance from the DC coefficient and according to the overall energy of the TB. The QP value is modified indirectly by modifying the corresponding multiplication factor (MF) value [1]. The MF is altered by utilizing a weight computed by an exponential function, which facilitates the *soft thresholding* mechanism. In contrast to URQ, SSIM, IDSQ, and AQSCV, our technique modifies QP values at the transform coefficient level instead of at the block level. The technique proposed in [6], although designed to work at the coefficient level, is restricted to a fixed number of QP values, which are mainly selected by taking into account the coefficient's position in the scan pattern. The fixed number of QPs is also true for SSIM, IDSQ and AQSCV because they are block level techniques.

We evaluate our technique on the reference encoder HM 16 [7] using the JCT-VC common test conditions [8]. Experimental evaluation results reveal important improvements, in terms of reconstruction quality, in all test sequences. Our method yields particularly high BD-Rate gains for Class E sequences encoded with the Low Delay B and Low Delay P configurations for both luma and chroma components.

The rest of the paper is organized as follows. Section 2 briefly describes the quantization process in HEVC. Section 3 discusses our proposed technique. Section 4 includes the experimental evaluations and computational complexity analysis, in which we compare our technique with reference encoder HM 16 and a related state-of-the-art technique. Finally, Section 5 concludes this paper.

This work was supported by the Engineering and Physical Sciences Research Council (EPSRC) of the United Kingdom. Reference: P83801G.

II. QUANTIZATION IN HEVC

Following intra or inter prediction, for each TB ranging from 4×4 to 32×32 samples, a finite precision approximation of the DCT is applied to the residual signal to compute the transform coefficients [9]. For intra predicted 4×4 luma TBs, a separable integer approximation of the Discrete Sine Transform (DST) is applied for all intra prediction modes [10]. In transform skip mode, the transform is bypassed in both intra and inter picture coding [2]. After linear transformation, a TB comprises low frequency components consisting of a DC coefficient and the AC coefficients close in proximity. It also includes high frequency components, which are the AC coefficients farthest from the DC coefficient. In both cases, proximity is measured in terms of Euclidean distance between positions within the TB. The energy of the TB is then concentrated in the low frequency components; for this reason, low frequency transform coefficients are more important than high frequency transform coefficients in terms of signal reconstruction and visual quality.

A transform coefficient $C(x,y)$, located at coordinates (x,y) within an $N\times N$ TB, is quantized to a transform coefficient level value l, as given by (1):

$$l(x,y) = \frac{C(x,y)\cdot Q + offset}{2^{21+\frac{QP}{6}-\log_2 N}} \quad (1)$$

where Q is the MF associated with the QP value and *offset* is a constant value that specifies the error caused by rounding and the level of deadzone [1]. At the decoder side, a transform coefficient is recovered by inverse quantization, as given by (2) [11]:

$$C'(x,y) = \frac{l(x,y)\cdot IQ \cdot 2^{\frac{QP}{6}}}{2^{\log_2 N - 1}} \quad (2)$$

where $C'(x,y)$ is the recovered coefficient located at coordinates (x,y) within an $N\times N$ TB and IQ is the scaling factor used for inverse quantization. Table 1 tabulates Q and IQ values for the first six, out of 52, QP values available in URQ. Note that in URQ, all coefficients in a TB are equally quantized and Q values are independent from the position of transform coefficients; therefore, a single QP value is used in a TB [6].

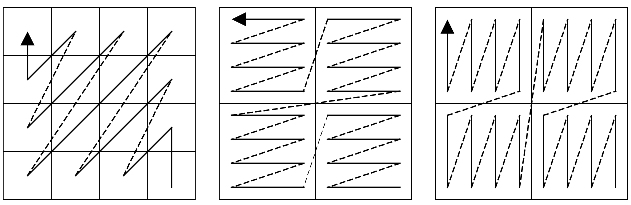

(a) (b) (c)

Fig. 1. (a) Diagonal reverse scan pattern used to process coefficients within a 4×4 TB. Horizontal (b) and vertical (c) reverse scan patterns for processing 4×4 Sub-Blocks (SBs) of 8×8 TBs and for processing SB frequency positions when intra prediction is used. Figures (b) and (c) show the case of a sample 8×8 TB with four 4×4 SBs.

Table 1. The first six of 52 QP values in URQ.

QP	0	1	2	3	4	5
Q	26214	23302	20560	18396	16384	14564
IQ	40	45	51	57	64	72

After quantization, the resulting l values are entropy coded by Context Adaptive Binary Arithmetic Coding (CABAC) following a specific scanning order, which exploits the fact that transform coefficient levels are concentrated in the top left region of the TB when using inter prediction and in the top or left border of the TB when using intra prediction [2]. The scanning order uses diagonal, horizontal or vertical reverse scan patterns depending on the prediction mode used, as illustrated in Fig. 1 [2].

III. PROPOSED QUANTIZATION TECHNIQUE

Our quantization technique is based on modifying the QP value at the coefficient level according to the importance of the transform coefficients in terms of reconstructing the signal. This may be achieved by defining a set of possible QP values for each TB and quantizing each coefficient using a specific QP value from this set via thresholding, where the threshold represents a specific level of importance. The use of continuous functions, where no hard decision is required, usually leads to improved results [12]. Therefore, our technique uses a continuous, monotonically decreasing function to define the importance of a transform coefficient in terms of reconstructing the signal. We have entitled this mechanism *soft thresholding*. Our technique employs a weight, w, quantified by an exponential function in (3):

$$w = e^{-\left(\frac{d}{c}\right)^2} \in [0,1] \quad (3)$$

where d is the normalized Euclidean distance between the positions of the current coefficient in the TB and the DC coefficient, and where c denotes the normalized total energy of the TB. Weight w modifies MF in (1) for both luma and chroma components in a TB as shown in (4):

$$Q' = Q \times w \quad (4)$$

where Q' represents the modified MF after weighting by w. The inverse quantization process is also modified accordingly, which equates to the following: $IQ'\times Q' = 2^{20}$ for both luma and chroma components. Note that applying weight w to Q results in the indirect modification of the QP value of a transform coefficient according to the coefficient's position in relation to its Euclidean distance from the low frequency components and also according to the overall energy of the TB. The distinct advantage of modifying the MF is as follows: the range of MF values is greater than the available range of QP values; therefore, this allows for adapting the MF value at a finer granularity level by combining the transform coefficient distance information and the overall energy of the TB. In addition, altering the MF to change the QP value has been shown to improve coding efficiency performance [6]. It is important to mention that weight w in (3) can be calculated for all TB sizes; it provides a specific QP value for each transform coefficient without having to measure multiple QP values using a hard thresholding approach. Therefore, our *soft thresholding* approach, within this context of quantization, refers to the idea of avoiding the selection of different thresholds that switch between two or more functions or values; that is, by employing soft decision thresholding as opposed to hard decision thresholding. More detailed explanations of parameters d and c involved in weight w are presented in the following sections.

DC *0* **0**	***AC*** *1.0000* **0.2357**	***AC*** *2.0000* **0.4714**	***AC*** *3.0000* **0.7071**
AC *1.0000* **0.2357**	***AC*** *1.4142* **0.3333**	***AC*** *2.2361* **0.5271**	***AC*** *3.1623* **0.7454**
AC *2.0000* **0.4714**	***AC*** *2.2361* **0.5271**	***AC*** *2.8284* **0.6667**	***AC*** *3.6056* **0.8499**
AC *3.0000* **0.7071**	***AC*** *3.1623* **0.7454**	***AC*** *3.6056* **0.8499**	***AC*** *4.2426* **1**

Fig. 2. Graphical representation of transform coefficients in a 4×4 TB. The positions of the low frequency components, including the DC coefficient, are displayed in darker shades. Numerical values represent the Euclidean distance of each coefficient from the DC coefficient before (italics) and after (bold) normalization.

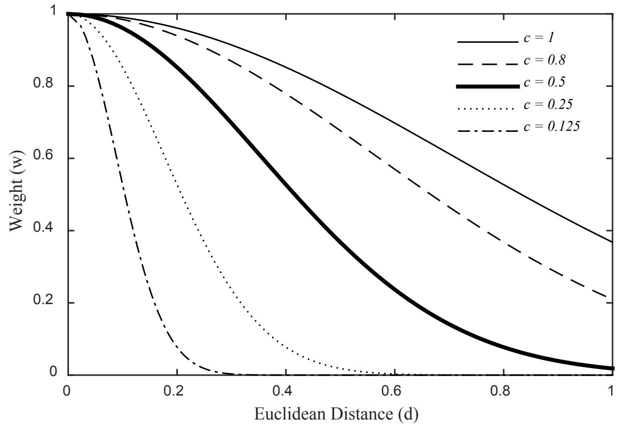

Fig. 3. Weight w for various values of the energy parameter c and Euclidean distance d. Note how c controls the exponential decay of w.

A. Distance Parameter

Figure 2 represents a sample 4×4 TB. The position of the DC coefficient is displayed in dark gray, the AC coefficients close in proximity to the DC coefficient are displayed in lighter gray, while the position of the AC coefficient farthest from the DC coefficient is displayed in white. This change in color (dark to light) represents the change, among the coefficients within a TB, in terms of frequency content (low to high), distance to the DC coefficient (small to large) and energy content (high to low). The distance parameter d takes into consideration how distant an AC coefficient is from the DC coefficient; therefore, it indirectly takes into account the frequency and energy content of the coefficient. Each coefficient is quantized at different levels according to its distance from the DC coefficient. For example, the low energy AC coefficient shown in white — bottom right in Fig. 2 — is quantized at a much higher level than the DC coefficient or the AC coefficients close in proximity to the DC coefficient. The Euclidean distance between two coefficients in an $N\times N$ TB is calculated and normalized in (5):

$$d = \sqrt{\frac{(x_1 - x_2)^2 + (y_1 - y_2)^2}{(x_1 - x_{\max})^2 + (y_1 - y_{\max})^2}} \in [0,1] \qquad (5)$$

where (x_1, y_1), (x_2, y_2) and $(x_{\max}, y_{\max})$ represent the (x,y) coordinates of the DC coefficient, the current coefficient and the farthest AC coefficient, respectively. The DC coefficient is at position $x = 1, y = 1$.

B. Energy Parameter

The energy parameter c in (3) controls the decay of the exponential function for the purpose of gradually decreasing MF values. This parameter is computed in (6):

$$c = \frac{E}{E_{\max}} \in [0,1] \qquad (6)$$

where E is an estimate of the total energy of an $N\times N$ TB and $E_{\max}$ is a constant that approximates the maximum energy value of the $N\times N$ TB. Let us denote the n^{th} recovered transform coefficients within an $N\times N$ TB as C'_n, with $n = 1$ and $n = N\times N$ denoting the DC coefficient and the coefficient located at the coordinates ($x=N$, $y=N$), respectively, following a zig-zag order. The value of E for the n^{th} coefficient in an $N\times N$ TB is computed in (7), as follows.

$$E_n = \sum_{m=1}^{n-1} (C'_m)^2 \qquad (7)$$

According to (7), the value of E for the n^{th} coefficient is quantified using the recovered value of the n-1 previously encoded coefficients, where the first coded coefficient is the DC coefficient. The purpose of E is to adapt weight w in (3) at a finer granularity level by combining it with the aforementioned distance information. Because the Q value is altered at the coefficient level based on distance and energy, this has the potential of enhancing the reconstruction quality of the signal.

The maximum energy value of the TB, $E_{\max}$, is utilized to normalize the energy value E. Calculating the exact maximum energy value of a TB *a priori* of the encoding process is usually not feasible; even if it is feasible, storing a specific $E_{\max}$ value for each TB would hinder the coding efficiency. Therefore, $E_{\max}$ is estimated in the frequency domain as the energy of an $N\times N$ TB in which all residual values are equal to $r = 2^b$-1, where b represents the bit depth of the data. The value of c in Eq. (6) is then clipped to the range [0,1].

Figure 3 shows the plot of weight w in (3) for various values of d and c. The plot shows that w slowly decays as c increases; that is, for those TBs with high energy values. For TBs with low energy values, w rapidly decays as d increases. In other words, w adapts to the importance of the transform coefficient in the signal reconstruction process.

The proposed technique is suitable for, and can be utilized with, the current scan patterns used for entropy coding (see Fig. 1) due to the fact that quantization is performed at the transform coefficient level using information about each coefficient and the whole TB; that is, the coefficient's proximity to the low frequency components and the overall energy of the TB. Therefore, transform coefficient levels still tend to be concentrated in the top left region of the TB when using inter prediction and in the top or left border of the TB when using intra prediction.

Table 2. Luma and chroma BD-Rate improvements of the proposed technique (compared with anchor) and the N-Level Quantizer [6] (compared with anchor) for classes A, B, C, D and E for the Low Delay B, Low Delay P, Random Access and All Intra configurations. A negative percentage indicates BD-Rate reductions. In [6], not all tests were conducted; "N/A" indicates the absence of tests. The row I-HM indicates average BD-Rate improvements of our technique and the N-Level Quantizer versus anchor. The row I-NQ indicates the average BD-Rate improvements of our technique compared with the N-Level Quantizer.

N-LEVEL QUANTIZER [6] VERSUS ANCHOR

Class	Low Delay B Main			Low Delay B HE		
	Y %	U %	V %	Y %	U %	V %
A	N/A	N/A	N/A	N/A	N/A	N/A
B	-0.7	-0.8	-1.0	-0.9	-2.1	-1.5
C	0.2	0.8	0.1	-0.2	0.2	-0.6
D	-0.1	-1.6	-1.7	-0.2	0.8	0.1
E	-0.2	-1.7	-1.3	-0.6	-2.4	-1.4
I-HM	**-0.3**	**-0.8**	**-0.9**	**-0.5**	**-1.1**	**-1.0**

Class	Low Delay P Main			Low Delay P HE		
	Y %	U %	V %	Y %	U %	V %
A	N/A	N/A	N/A	N/A	N/A	N/A
B	-0.9	0.0	-1.2	-0.8	-2.2	-1.8
C	0.1	0.9	-0.1	0.0	0.4	-0.4
D	-0.3	-2.5	0.0	-0.2	0.5	-0.5
E	-0.2	-1.3	-1.5	-0.2	-1.6	-1.2
I-HM	**-0.4**	**-0.6**	**-0.8**	**-0.5**	**-1.3**	**-1.2**

Class	Random Access Main			Random Access HE		
	Y %	U %	V %	Y %	U %	V %
A	N/A	N/A	N/A	N/A	N/A	N/A
B	N/A	N/A	N/A	N/A	N/A	N/A
C	N/A	N/A	N/A	N/A	N/A	N/A
D	N/A	N/A	N/A	N/A	N/A	N/A
E	N/A	N/A	N/A	N/A	N/A	N/A
I-HM	N/A	N/A	N/A	N/A	N/A	N/A

Class	All Intra Main			All Intra HE		
	Y %	U %	V %	Y %	U %	V %
A	-0.7	1.9	3.9	-0.2	-0.6	1.1
B	-0.3	-1.9	-2.3	-0.4	-2.4	-2.9
C	-0.5	-0.6	-0.5	-0.6	-0.7	-0.6
D	-0.1	-1.0	-1.4	-0.2	-0.4	-0.2
E	0.0	-2.3	-2.7	0.0	-3.3	-3.0
I-HM	**-0.4**	**-0.5**	**-0.2**	**-0.3**	**-1.5**	**-1.1**

PROPOSED TECHNIQUE VERSUS ANCHOR

Class	Low Delay B Main			Low Delay B HE		
	Y %	U %	V %	Y %	U %	V %
A	-3.4	-7.4	-9.3	-3.7	-7.1	-8.7
B	-2.1	-8.5	-9.7	-2.0	-8.8	-9.4
C	-2.4	-6.5	-6.8	-2.3	-6.7	-6.5
D	-1.9	-8.4	-8.0	-1.6	-8.4	-8.9
E	-5.5	-13.2	-11.7	-5.0	-12.4	-11.8
I-HM	**-3.0**	**-8.8**	**-9.1**	**-2.9**	**-8.7**	**-9.1**
I-NQ	**-2.7**	**-8.0**	**-8.2**	**-2.4**	**-7.6**	**-8.1**

Class	Low Delay P Main			Low Delay P HE		
	Y %	U %	V %	Y %	U %	V %
A	-3.6	-7.1	-9.4	-3.9	-6.8	-9.1
B	-2.1	-8.4	-9.6	-2.1	-7.8	-9.3
C	-2.6	-7.0	-7.0	-2.6	-7.1	-7.1
D	-1.9	-8.8	-7.5	-1.9	-8.1	-8.1
E	-5.4	-13.6	-12.4	-5.4	-13.3	-11.9
I-HM	**-3.1**	**-9.0**	**-9.2**	**-3.2**	**-8.6**	**-9.1**
I-NQ	**-2.7**	**-8.4**	**-8.4**	**-2.7**	**-7.3**	**-7.9**

Class	Random Access Main			Random Access HE		
	Y %	U %	V %	Y %	U %	V %
A	-0.8	1.9	1.0	-0.8	2.1	0.6
B	-0.2	-0.6	-0.9	-0.2	-0.4	-1.1
C	-0.2	-2.0	-1.0	-0.2	-0.8	-1.0
D	0.1	-1.1	-0.9	0.1	-0.9	-1.1
E	-0.2	-0.7	-1.0	-0.3	-0.7	-0.6
I-HM	**-0.2**	**-0.5**	**-0.6**	**-0.3**	**-0.2**	**-0.6**

Class	All Intra Main			All Intra HE		
	Y %	U %	V %	Y %	U %	V %
A	-0.2	-0.2	-0.6	-0.2	-0.2	-0.7
B	-0.1	-0.4	-0.4	-0.1	-0.3	-0.5
C	0.1	-0.3	-0.4	0.0	-0.3	-0.4
D	0.1	-0.4	-0.3	0.1	-0.3	-0.3
E	-0.2	-0.2	-0.1	-0.2	-0.2	-0.1
I-HM	**-0.1**	**-0.3**	**-0.4**	**-0.1**	**-0.3**	**-0.4**
I-NQ	**0.3**	**0.2**	**-0.2**	**0.2**	**1.2**	**0.7**

IV. EXPERIMENTAL EVALUATION

A. Test Conditions

We evaluate our technique with the common test conditions recommended by JCT-VC [8]. The official test sequences have resolutions of 2560×1600, 1920×1080, 832×480, 416×240 and 1280×720, which represent classes A, B, C, D and E, respectively. All frames of each sequence are encoded with the following configurations: All Intra, Low Delay B, Low Delay P and Random Access using the Main Profile (MP), the High Efficiency (HE) profile and the QP values: 22, 27, 32 and 37. CABAC is the entropy coding method used for both profiles. The RDOQ encoder option and transform skip mode are disabled in all tests for the reference encoder and our technique. In the All Intra configuration, sequences are encoded using only I-frames, for which all three reverse scan patterns (horizontal, vertical and diagonal) are used (see Fig. 1). The Low Delay B and Low Delay P configurations encode all sequences with B-frames and P-frames, respectively. The Random Access configuration also encodes the sequences with B-frames; however, the Group of Pictures (GOP) structure is more complex in comparison with the Low Delay configurations [7]. In the Low Delay B, Low Delay P and Random Access configurations, inter predicted blocks use only the reverse diagonal scan pattern.

The proposed technique is compared with anchor reference encoder HM 16 [7] and the N-level Quantizer technique proposed in [6], which is the HEVC quantization contribution most similar to our method. The N-Level Quantizer employs N = 3 levels of quantization, which are selected according to the scan pattern of a TB and the scan position of the transform coefficients.

All tests of our technique were conducted on a 3.4 GHz Intel Core i7-4770 (four physical cores) machine with 32 GB of RAM, on which Windows 7 Professional 64-bit is installed.

B. Experimental Results Summary & Discussion

On the right hand section in Table 2, we tabulate the average BD-Rate enhancements of our method compared with the anchor reference encoder HM 16 for all configurations and sequences in each class. These results are compared with the average BD-Rate improvements of the N-Level Quantizer, which are shown on the left section in Table 2 as reported in [6]. We also compare the average BD-Rate gains of our novel technique versus the average BD-Rate gains of the N-Level Quantizer. BD-Rate improvements are calculated as the change in bitrate when the reconstruction quality, measured by the Peak Signal to Noise Ratio (PSNR) metric, is the same [13]. Negative percentages indicate BD-Rate reductions.

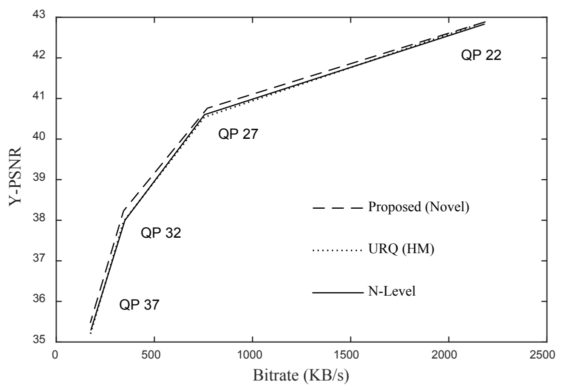

Fig. 4. RD-Plot showing the Y-PSNR improvements of our technique compared with URQ and the N-Level Quantizer for the sequence *KristenAndSara* in Class E using the Low Delay B Main configuration.

As shown on the right in Table 2, in comparison with the anchor reference encoder HM 16, the most noteworthy luma and chroma BD-Rate gains attained by our technique are as follows: -5.5% (Y), -13.2% (Cb) and -11.7% (Cr) for HD sequences in Class E using the Low Delay B configuration and Main profile. In comparison with the N-Level Quantizer, the most significant average luma and chroma BD-Rate improvements achieved by our method are as follows: -2.7% (Y), -8.4% (Cb) and -8.4% (Cr) using the Low Delay P configuration and Main profile. Figure 4 shows an RD-Plot for the *KristenAndSara* sequence in Class E, which yields BD-Rate gains of -6.4% for Y-PSNR. In terms of individual class of sequence and the performance of our method in comparison with anchor, our technique performs particularly well on the inter predicted residual transform coefficients in Class E sequences. The reason for this is as follows: in these sequences, the inter predicted residual values are low and, as a consequence, the majority of the TBs are low in energy. Therefore, our technique adaptively utilizes high QP values for the low energy transform coefficients in these TBs.

Because of the BD-Rate improvements that our adaptive quantization technique attains, we can assert that quantization at the transform coefficient level — taking into account transform coefficient distance information and TB energy — produces improved coding efficiency in comparison with the default block level quantization procedure (URQ). Our technique proves that by taking into account the importance of each transform coefficient and the entire TB in the signal reconstruction process, efficient quantization schemes can be designed.

C. Complexity Analysis & Discussion

We next analyze the impact of our quantization scheme on the overall encoding and decoding times. The computational complexity of our technique, URQ and the N-Level Quantizer can be computed using linear time, given by (8):

$$T(n) = O(n) \quad (8)$$

That is, the computational performance of these scalar quantization techniques is directly proportional to the number of transform coefficients being processed in each TB. Although URQ is a block based quantization technique, it processes transform coefficients individually in each TB using (1); however, with URQ each coefficient is quantized equally according to a QP. In contrast, our technique modifies the MF in (1) with (3). This refinement of (1) with (3) does not increase computational complexity, which is evidenced by the modest decrease in encoding and decoding times of our technique for sequences in which the majority of TBs are low in energy.

Our technique reduces the number of non-zero quantized transform coefficients. This results in faster entropy coding and decoding times. Furthermore, fewer non-zero coefficients results in an encoded bitstream with fewer bits compared with URQ in the vast majority of cases. Figure 5 shows a plot of the improved encoding time performance of our method; Table 3 tabulates the improved encoding time and decoding time performance of our technique for five HD sequences. Moreover, Table 3 indicates that our approach yields maximum speed improvements of 3.6% and 11.5% for encoding and decoding, respectively.

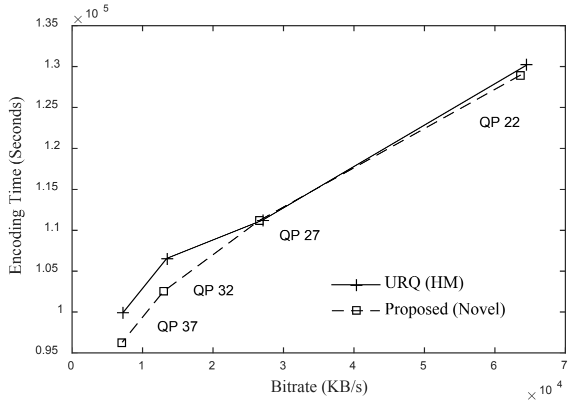

Fig. 5. Plot showing the improved encoding time performance of our technique compared with URQ for all sequences and configurations specified in Table 3.

Table 3. The improved average encoding time and decoding time (seconds) improvements of our technique compared with URQ for five HD sequences. The sequences are: *BasketBallDrive*, *PeopleOnStreet*, *Johnny, FourPeople* and *KristenAndSara* using the Low Delay B Main configuration simulations for QPs 22, 27, 32 and 37.

	QP 22	**QP 27**	**QP 32**	**QP 37**
URQ Encoding Times	130166	111239	106555	99924
URQ Decoding Times	197	146	123	113
Novel Encoding Times	128982	111168	102526	96298
Novel Decoding Times	192	145	122	100
Novel Encoding Gains	**-0.9%**	**-0.1%**	**-3.8%**	**-3.6%**
Novel Decoding Gains	**-2.5%**	**-0.7%**	**-0.8%**	**-11.5%**

V. CONCLUSION

In this paper, we have presented an adaptive soft thresholding quantization method for HEVC. We have proposed a transform coefficient level method of quantization that takes into consideration the importance of the transform coefficients in the signal reconstruction process; namely, the amount of information conveyed by the coefficients and the overall energy in the corresponding TB. We compared our technique with URQ and a recently proposed coefficient level quantization technique entitled N-Level Quantizer. Performance evaluations revealed that our technique produces appreciable BD-Rate improvements, particularly for Class E sequences, with BD-Rate reductions of up to 5.5% (Y), 13.2% (Cb) and 11.7% (Cr) in addition to modest decreases in encoding and decoding times.

REFERENCES

[1] G. Sullivan, J-R. Ohm, W. Han and T. Wiegand, “Overview of the High Efficiency Video Coding (HEVC) Standard,” *IEEE Trans. Circuits Syst. Video Technol*., vol. 22, no. 12, pp. 1649-1668, 2012.

[2] T. Nguyen et al., “Transform Coding Techniques in HEVC,” *IEEE J. Sel. Topics Signal Process*., vol. 7, no. 6, pp. 978- 989, Dec. 2013.

[3] Y. Chuohao, T. Hui Li and T. Yih Han, “SSIM-Based Adaptive Quantization in HEVC,” *IEEE Int. Conf. Acoustics, Speech and Signal Processing*, Vancouver, BC, 2013, pp. 1690-1694.

[4] M. Naccari and M. Mrak, “Intensity Dependent Spatial Quantization with Application in HEVC,” *IEEE Int. Conf. Multimedia and Expo*, San Jose, CA, 2013, pp. 1-6.

[5] J. Nam, D. Sim and I.V. Bajic, “HEVC-based Adaptive Quantization for Screen Content Videos,” *IEEE Int. Symp. Broadband Multimedia Systems*, Seoul, 2012, pp. 1-4.

[6] R. Gweon and Y. Lee, “N-Level Quantization in HEVC,” *IEEE Int. Symp. Broadband Multimedia Systems*, Seoul, 2012, pp. 1-5.

[7] Joint Collaborative Team on Video Coding (2014). HEVC Reference Software, HM 14.0 [Online]. Available: http://hevc.hhi.fraunhofer.de/

[8] F. Bossen, “Common Test Conditions and Software Reference Configurations,” *JCTVC-L1100*, 2013, pp. 1–4.

[9] M. Budagavi et al., “Core Transform Design in the High Efficiency Video Coding (HEVC) Standard,” *IEEE J. Sel. Topics Signal Process*., vol. 7, no. 6, pp. 1649-1668, Dec. 2013.

[10] A. Fuldseth et al., “Transform design for HEVC with 16 bit intermediate data representation,” *JCTVC-E243*, 2011, pp. 1–16.

[11] J. Sole et al., “Transform Coefficient Coding in HEVC,” *IEEE Trans. Circuits Syst. Video Technol*., vol. 22, no. 12, pp. 1765-1777, 2012.

[12] V. Sanchez, R. Abugharbieh and P. Nasiopoulos, “3D Scalable Medical Image Compression with Optimized Volume of Interest Coding,” *IEEE Trans. Med. Imag*., vol. 29, no. 10, pp. 1808-1820, Oct. 2010.